MRS Advances © 2016 Materials Research Society
DOI: 10.1557/adv.2016.198

Quasi-Continuously Tuning the Size of Graphene Quantum Dots via an Edge-Etching Mechanism

Shujun Wang[1,2], Ivan S. Cole[3] , Dongyuan Zhao[4], and Qin Li[1,2*]

[1]Queensland Miro- and Nanotechnology Centre, Griffith University, Nathan Campus, Brisbane, QLD 4111, Australia
[2]School of Engineering (Environmental), Griffith University, Nathan Campus, Brisbane, QLD 4111, Australia
[3]CSIRO Materials Science and Engineering, –Gate 5, Normanby Road, Clayton, VIC 3168, Australia
[4] Department of Chemistry & Laboratory of Advanced Materials, Fudan University, Shanghai, 200433, P.R. China
*Corresponding author at: Nathan campus Griffith University,170 Kessels Road, Nathan, QLD 4111, Au; E-mail address: qinli@griffith.edu.au; Tel.: (07) 373 57514

ABSTRACT

Graphene quantum dots (GQDs), a nano version of graphene whose interesting properties that distinguish them from bulk graphene, have recently received significant scientific attention. The quantum confinement effect referring to the size-dependence of physical and chemical properties opens great possibility in the practical applications of this material. However, tuning the size of graphene quantum dots is still difficult to achieve. Here, an edge-etching mechanism which is able to tune the size of GQDs in a quasi-continuous manner is discovered. Different from the 'unzipping' mechanism which has been adopted to cut bulk graphitic materials into small fragments and normally cut through the basal plane along the 'zig-zag' direction where epoxy groups reside, the mechanism discovered in this research could gradually remove the peripheral carbon atoms of nano-scaled graphene (i.e. GQDs) due to the higher chemical reactivity of the edge carbon atoms than that of inner carbon atoms thereby tuning the size of GQDs in a quasi-continuous fashion. It enables the facile manipulate of the size and properties of GQDs through controlling merely the reaction duration. It is also believed the as discovered mechanism could be generalized for synthesizing various sizes of GQDs from other graphitic precursors (e.g. carbon fibres, carbon nanotubes, etc).

INTRODUCTION

Recently, a nano-scaled carbon material, graphene quantum dots (GQDs) referring to graphene fragments or discs normally having lateral size less than 100nm [1] has been attracting increasing attention in a variety of fields including single-electron transistors [2-4], spintronics [5, 6], energy conversion [7, 8], memory [9, 10], optoelectronics [11], sensing [12-15] and bioimaging [16-20] etc. The emergence of this material could be attributed to its interesting properties such as tuneable electronic and magnetic properties, photoluminescence, low cytotoxity1 [21-27], etc. that distinguish themselves from bulk graphene.

Although GQDs have been investigated theoretically even before the discovery of graphene [25], experimental synthesis of this material is just a recent effort. So far, a variety of methods have been developed to synthesize GQDs. These methods could be assigned to one of the two groups of methods which either take a top-down strategy involving breaking bulk graphitic materials into GQDs [28-32] or follow a bottom-up mindset trying to construct GQDs from molecules [8, 33, 34]. Through these methods various types of GQDs have been made available.

However, all the GQDs preparation methods developed so far share a same shortcoming that is the lack of easy tuneability of the size of GQDs. Size tuneability is essential to the fundamental study and application potential of GQDs, because the aforementioned excellent properties are all size-dependent. For instance, the rise of band gaps for GQDs is due to quantum confinement which is size dependent [1], Theoretical studies have indicated that the band gap of GQDs should become wider with the decrease of lateral size, vice versa [24, 35]. The top-down approaches usually result in broad size distribution, only one to three GQDs with different average particle sizes could be made available in most of the existing publications [28-32, 36, 37]. Bottom up methods are considered to be more controllable method in terms of tuning particle size, indeed, through method such as microwave assisted hydrothermal synthesis, certain degree of tuneability of particle size could be achieved [38]. However, the tuneability is limited by the abrupt increase of size with small variation of tuning condition. Hence, a method which could provide better control and near continuous tuneability of size of GQDs is still absent.

Here we report an edge etching mechanism through which quasi-continuous tuneability of size of GQDs could be realized. Synthesis of GQDs and tuning their size was achieved in a one-pot set up in this study. A mixed acid approach was adopted for synthesis of graphene quantum dots by dismantling and exfoliating carbon black (CB) which contains nano-sized graphitic crystallites (lateral size ~3nm, 7~9 layers carbon atoms). After the dismantling and exfoliation, the size of resulting GQDs could be near continuously reduced via the edge etching mechanism which is able to continuously remove the edge carbon atoms over time. Therefore, the size of GQDs could be tuned simply by changing the reaction duration. To the best of our knowledge, this is the first method that could achieve near continuous and easy tuneability of size of GQDs.

EXPERIMENTAL

Synthesis of GQDs from carbon black

50 mg of carbon black (Spuer P, Alfa Aesar) was put inside a 50 ml round flask. 6 ml of concentrated HNO_3 (70%, Chem-Supply) was then introduced to the round flask followed by adding 18 ml H_2SO_4 (98%, Chem-Supply) slowly and carefully under magnetic stirring (350 rpm). Upon the completion of adding the materials, the round flask was placed into a silicon oil bath with temperature set as 160˚C. A condenser was subsequently applied to reflux the vapourized acids and acids decompositions (majorly HNO_3 decompositions since gas with brown colour were generated inside round flask) and the reflux is quite critical, because without it nitric acid would fully decompose too quickly, resulting in termination of reaction. Upon completion of reaction for targeted duration, the reacted materials were poured slowly into 200 mL of DI water under vigorous stirring. NaOH (Chem-Supply) pellettes were added slowly till PH=5.

Then the PH of the solution was further tuned to 7 via a NaOH solution (100 mg/ml). The final solution was subsequently concentrated to 100 ml before subject to dialysis with a 500 Da tube membrane (SpectrumLabs) for 3 days. Upon completion of the dialysis the purified GQDs solution inside the tube membrane was collected.

Characterization

High resolution transmission electron microscope (HRTEM, Philips Tecnai F20), along with atomic force microscope (AFM, NT-MDT NTEGRA Spectra) were adopted for the morphology analysis. Fluorescent spectra were collected through a fluorescence spectrometer (Thermo Scientific Lumina). Raman spectra were obtained via a Raman spectrometer (Renishaw) with a 514 nm laser source. Elemental compositions and chemical bonding status were quantitatively analysed by X-ray photoelectron spectroscopy (XPS, Kratos Axis Ultra).

RESULTS AND DISCUSSION

Synthesis of GQDs from carbon black

Previous X-Ray Diffraction (XRD) studies have shown that carbon black is composed of layered sp^2 crystallites (graphitic structure) which are assembled together in random orientations, forming clusters in the appearance of spheres, and the lateral sizes of those sp^2 crystallites are a few nano meters [39, 40]. Therefore, if the clustered sp^2 crystallites are dismantled and further exfoliated, the resulting product will be GQDs. Figure 1 a shows the carbon black adopted in this research. The dimensions of the crystallites in CB could be revealed by XRD through the Scherrer equation [39, 41, 42] and Raman spectroscopy via the Tuinstra-Koenig relationship [43] (see supplementary information for details of calculation). Briefly, two typical characteristic peaks were observed on the XRD spectra, namely, a peak around 25˚ which is due to the diffraction of 002 plane and the other peak around 44˚ which is due to the two dimensional diffraction of 10. The calculated lattice parameter c of the sp^2 crystallites is around 7.1A which is slightly larger than graphite (6.7A) and in consistent to existing literature [39]. The lateral size of the sp^2 crystallites (La) are calculated from both the 10 diffraction peak of XRD spectra and Raman spectra (Fig.S1). The values are roughly in good agreement (~3nm). The vertical size (Lc) of the sp^2 crystallites along c direction (i.e. the stacking direction) is around 2nm which could be translated into 7~9 layers of carbon atoms. The dismantling and exfoliation of CB was achieved by treating CB in mixed acids (Vol HNO_3/Vol H_2SO_4= 1:3) at 160˚C. Exfoliation of the sp^2 crystallites could be achieved in as short as 20 min. The morphology of GQDs obtained after reaction for 20min is presented in Figure 1 b and c. The average lateral size of the corresponding GQD is around 2 nm. AFM height profiles reveals the average thickness of the GQDs is around 1.2 nm, which could be translated into 1 or 2 layers of carbon atoms for such type of oxygenated GQDs, confirming the successful exfoliation of the sp^2 crystallites (originally 7~9 layers of carbon atoms) in CB. Moreover, over 60% of the resulting particles have the thickness less than or equal to 1.2nm, suggesting the high yield feature of the method. The as synthesized GQDs could be dispersed into water thoroughly to form solutions which are

extremely stable. No precipitation could be observed after the solutions were kept under room temperature for a period of seven month.

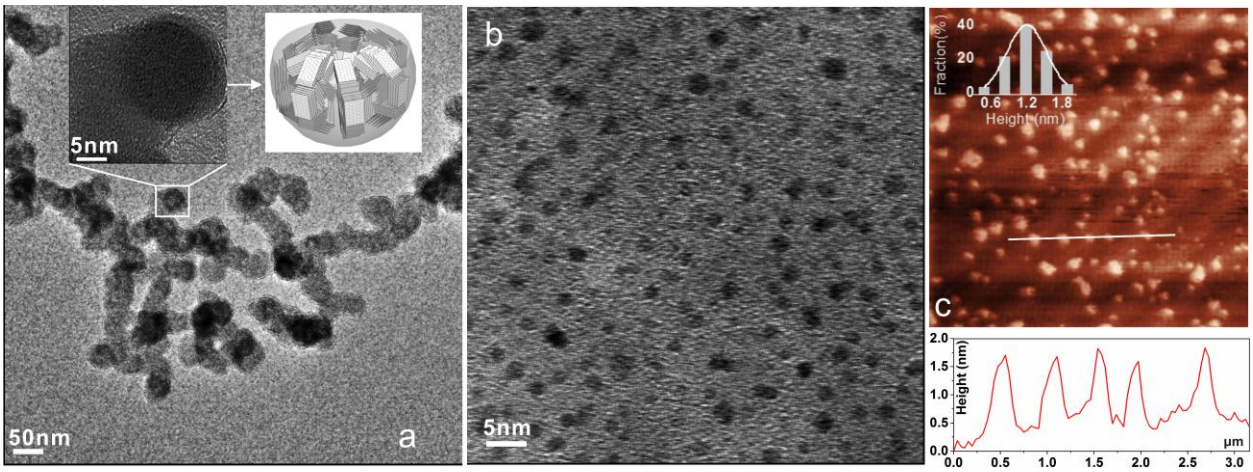

Figure 1. Morphology: HRTEM images of CB (a), the left inset is the high magnification image of a selected carbon black sphere, the right inset is a 3D graphical model of carbon black sphere; HRTEM (b) and AFM (c) images of G20, Inset in c is the height profile distribution of G20 derived from 300dots, Figure beneath c is the height profile along the line mark in c.

Quasi-continuously tuning the size of GQDs

The as synthesized GQDs possess excitation dependent photoluminescence (Fig. S 2). With extending the reaction duration (from here on all GQDs in this research are denoted such as G20, G80, G210 for which the numbers next to G indicate the durations taken for synthesizing the corresponding GQDs), a continuous blue shift trend was observed when the excitation was fixed at 340nm (Fig. 2 a). Such a blue shift feature is a prominent indication of quantum confinement effect or size effect, in which the smaller the particle size, the wider the band gap and the higher the emission energy (i.e. emission with shorter wavelength) [24,35]. Indeed, as confirmed by the Raman (Fig. S3 and Table S 1) and dynamic light scattering (DLS, Fig. 2 and Fig. S 4) measurements, the particle size gradually decreased with extending the reaction duration from 20min to 210min (Fig. 2 b). Hence, with extending the reaction duration this method could tune the size of GQDs in a quasi-continuous manner as indicated by the quasi continuous blue shift feature of PL spectra.

Edge etching mechanism

'Unzipping' mechanism [31, 32, 44, 45] has been believed to be responsible for cutting bulk graphitic materials (e.g. chemically reduced graphene oxide, graphite, carbon tube etc) into small species. This mechanism normally cut through the basal plane of large sheet structure along the 'zig-zag' direction where epoxy groups or carbonyl groups reside. However, based on the observation that the as-synthesized GQDs size quasi-continuously change as the reaction time extends, we deduce that the dominant particle size reduction mechanism in this reaction with carbon black as the parent material is edge-etching instead of unzipping, because cutting

through basal plane will result in abrupt change in size of the resultant species rather than reducing the size in a quasi-continuous manner. Since nano-sized graphene possess properties

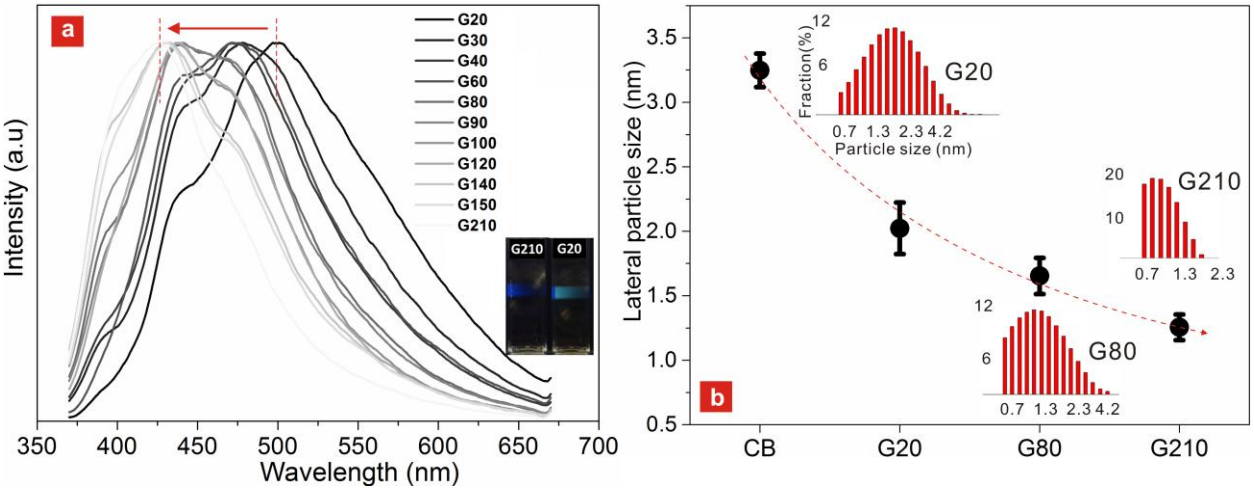

Figure 2. PL spectra of as synthesized GQDs under 340nm excitation (a) and lateral sizes of crystallites in CB and as synthesized GQDs (b). Insets in (a) are photos showing the photoluminescence of G20 and G210; Insets in (b) are the particle size distribution from DLS, data below 0.3nm could not be collected due to the instrument detection limit.

different from the ones either bulk graphene, or bulk graphitic materials have, we believe the size also play a decisive role in the chemical reactivity of GQDs. Indeed, previous studies have shown that nano-scaled graphene possess much higher chemical reactivity around edge than on the inner plane [46, 47]. In particular, through theoretic approach, Sheka et al. have suggested that, for nano-sized graphene, any chemical added will be firstly attached to the edge irrespective of edge terminations rather than the inner atoms on the basal plane [46]. Therefore, we postulate that a mechanism that is able to continuously etch away the edge atoms of GQDs, thereby reducing the size of particle in a quasi-continuous manner, should be responsible for the size tuneability of this study. In order to confirm this, we conducted a detailed quantitative analysis on the chemical composition change of the GQDs with the extension of reaction duration.

Figure 3 presents the fitted spectra of XPS and the corresponding summary from the peak fitting procedure. Similar to oxygenated GQDs synthesized from mixed acids oxidation method, the GQDs from this study also contain various types of oxygen functionalities represented by each of the Gaussion-Lorentzian component (%Guassion=30%) including hydroxyl, epoxy, carbonyl and carboxyl (Fig. 3 a). A notable feature is that the GQDs of this research possess similar carbon/oxygen ratio ~3 (3.0 for G20, 2.9 for G80, 3.2 for G210) indicating similar degree of oxidation (circular in Fig.3 b), which also suggests that the blue shift of PL spectrum as shown in Figure 2 could not result from change of degree of oxidation, confirming that the reduction of size is the dominated factor for the PL blue shift.

The quantitative variation of functional groups was further examined in detail (Fig. 3 b). On one hand, the atomic percentage of C-O (representing epoxy and hydroxyl) increased from 9% in G20 to 18% in G80 then dropped to 9.1% in G210; on the other hand, -C=O (representing carboxyl and carbonyl) decreased from 11.7% in G20 to 9.4% in G80 subsequently increased to 12.6% in G210. From the trends, it could be interpreted that the acids mixture firstly introduces

hydroxyl (to the edge) and epoxy (on the basal plane) to GQD which accounts for the percentage rise of C-O from G20 to G80, then converts hydroxyl into carboxyl and carbonyl on the edge,

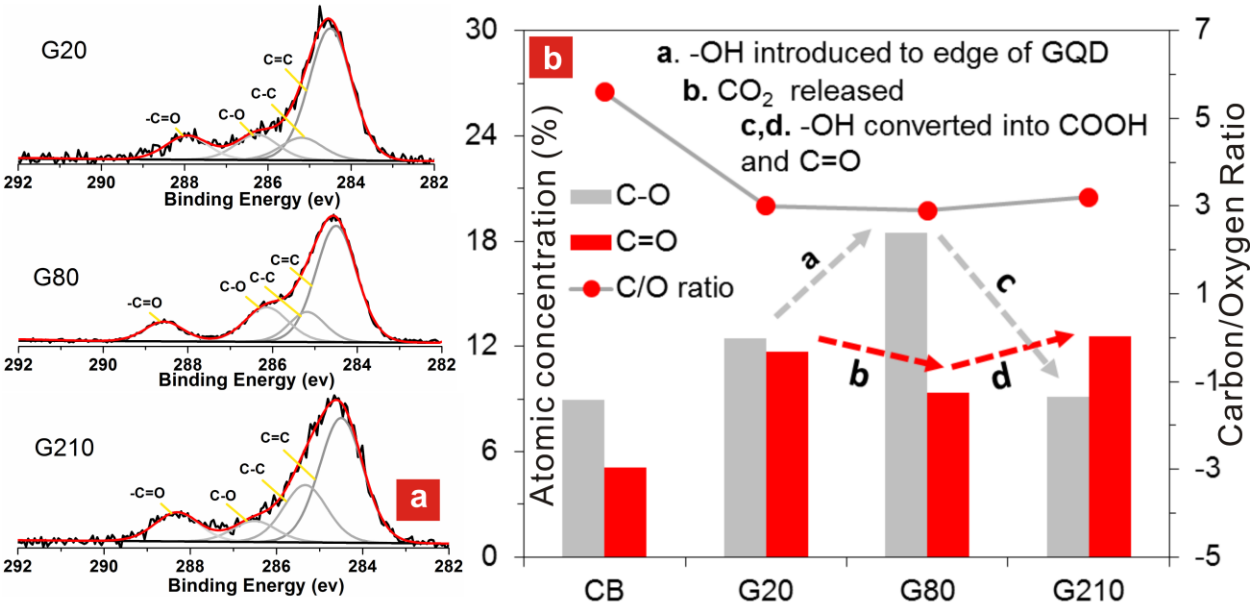

Figure 3. XPS results: (a) the fitted XPS spectra for G20, G80 and G210; (b) the quantitative summary of the chemical changes derived from XPS peak fitting

which accounts for the percentage drop of C-O and the percentage rise of –C=O from G80 to G210. However, the percentage increase of –C=O (~3%) did not compensate fully the percentage drop of C-O (~9%). This suggests there could be some other conversion coexisting which is able to consume C-O during the reaction. A highly likely conversion coexisting in the strongly oxidizing environment could be the complete oxidation converting –C=O into CO2, such a conversion would eventually fulfil the continuous removal of carbon atoms at the edge of GQDs.

Therefore, we deduce that an edge etching mechanism as illustrated in Figure 4 is responsible for the high tuneability of size of GQDs based on the above analysis; At the early stage (less than 20min) of this one pot reaction, CB spheres are dismantled and exfoliated into GQDs of original sizes. The strongly oxidizing environment then introduces considerable amount of hydroxyl to the edge of GQDs and few epoxy to the basal plane. The hydroxyl groups are further oxidized into carboxyl and carbonyl groups, breaking the sp^2 bonds of the peripheral carbon atoms. Carboxyl and carbonyl groups are eventually fully oxidized into CO_2 thereby removing the peripheral carbon atoms, which results in the size reduction of GQD. This dynamic reaction takes place in cycles, namely, once the outmost carbon atoms are removed, the carbon atoms next to them are exposed to the oxidizing environment which starts the next cycle of reaction. Through this dynamic repeating process, the size of GQD is tuned near continuously.

CONCLUSIONS

For the first time, a mechanism which is able to tune the size of graphene quantum dots in a quasi-continuous manner has been discovered. Different from cutting bulk graphitic materials into GQDs with similar oxidation approach, an edge etching mechanism for nano-sized graphene

is responsible for the supreme size tuneability achieved in this study. Fundamentally, the edge etching mechanism is caused by the fact that the chemical reactivity of the edge carbon atoms of nano-sized graphene (GQDs) is higher than that of inner carbon atoms on the basal plane as predicted by theoretical research [46, 47]. Such a difference in chemical reactivity leads to the preference of oxidation reactions to occur on the edge of GQDs, thereby quasi-continuously reducing the size of GQDs. It is believed the as discovered edge etching mechanism could also be applied to synthesize GQDs from other nano graphitic precursors for achieving a precise control of GQDs size, which is highly important for the fundamental research of nanocarbons and future applications in advanced optics and nanoelectronics.

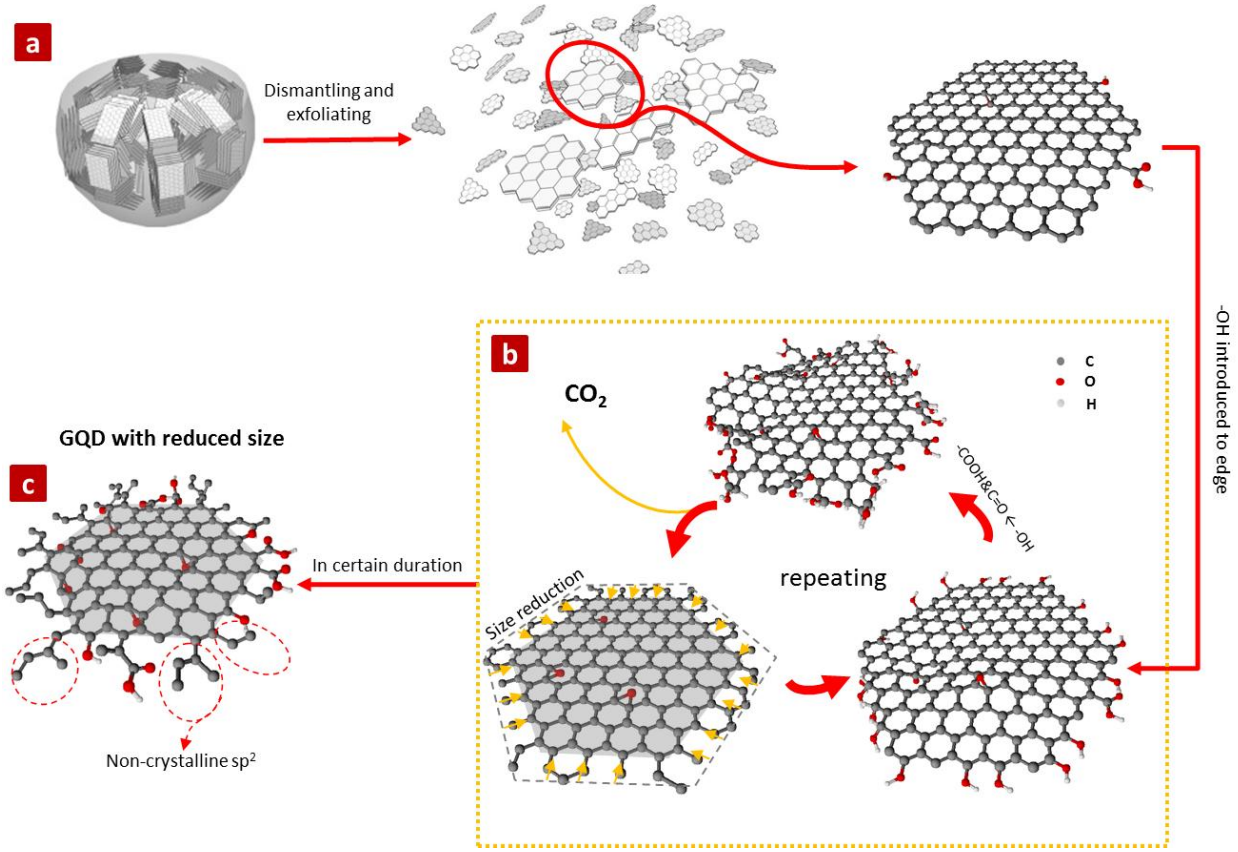

Figure 4. Schematic representation of the mechanism by which the high tuneability of size is realized: (a) dismantling and exfoliation of CB into GQDs of original size; (b), the oxidative environment firstly introduces hydroxyl to the edge of GQDs further convert hydroxyl into carboxyl and eventually removes peripheral carbon atoms via turning carboxyl into carbon dioxide; (c) With the reaction described in b repeating overtime, the size of GQD is gradually reduced.

ACKNOWLEDGMENTS

S.W. acknowledges the support of a Griffith International Postgraduate Scholarship (GIPS) and a CSIRO OCE top-up scholarship. Q.L. wishes to thank a Griffith University

Research Infrastructure Grant (GURIP). The authors wish to thank the Queensland Miro- and Nanotechnology Centre for the support.

REFERENCES

1. L. A. Ponomarenko, F. Schedin, M. I. Katsnelson, R. Yang, E. W. Hill, K. S. Novoselov and A. K. Geim, Science **320** (5874), 356-358 (2008).
2. A. Barreiro, H. S. van der Zant and L. M. Vandersypen, Nano letters **12** (12), 6096-6100 (2012).
3. T. Ihn, J. Guttinger, F. Molitor, S. Schnez, E. Schurtenberger, A. Jacobsen, S. Hellmuller, T. Frey, S. Droscher, C. Stampfer and K. Ensslin, Mater Today **13** (3), 44-50 (2010).
4. C. Stampfer, E. Schurtenberger, F. Molitor, J. Guttinger, T. Ihn and K. Ensslin, Nano letters **8** (8), 2378-2383 (2008).
5. M. Ezawa, New Journal of Physics **11** (9), 095005 (2009).
6. M. Ezawa, The European Physical Journal B **67** (4), 543-549 (2009).
7. Y. Wang, L. Zhang, R.-P. Liang, J.-M. Bai and J.-D. Qiu, Analytical chemistry **85** (19), 9148-9155 (2013).
8. X. Yan, X. Cui, B. Li and L. S. Li, Nano letters **10** (5), 1869-1873 (2010).
9. L. Kou, F. Li, W. Chen and T. Guo, Organic Electronics **14** (6), 1447-1451 (2013).
10. L. Zhao and S. F. Yelin, Physical Review B **81** (11) (2010).
11. J. Shen, Y. Zhu, X. Yang and C. Li, Chemical communications **48** (31), 3686-3699 (2012).
12. T. S. Sreeprasad, A. A. Rodriguez, J. Colston, A. Graham, E. Shishkin, V. Pallem and V. Berry, Nano letters **13** (4), 1757-1763 (2013).
13. H. Sun, N. Gao, L. Wu, J. Ren, W. Wei and X. Qu, Chemistry **19** (40), 13362-13368 (2013).
14. A. X. Zheng, Z. X. Cong, J. R. Wang, J. Li, H. H. Yang and G. N. Chen, Biosensors & bioelectronics **49**, 519-524 (2013).
15. S. J. Wang, Z. Lemon, I. S. Cole and Q. Li, Rsc Advances **5** (51), 41248-41254 (2015).
16. X. Sun, Z. Liu, K. Welsher, J. T. Robinson, A. Goodwin, S. Zaric and H. Dai, Nano research **1** (3), 203-212 (2008).
17. X. Wu, F. Tian, W. Wang, J. Chen, M. Wu and J. X. Zhao, Journal of materials chemistry. C, Materials for optical and electronic devices **1** (31), 4676-4684 (2013).
18. M. Zhang, L. Bai, W. Shang, W. Xie, H. Ma, Y. Fu, D. Fang, H. Sun, L. Fan, M. Han, C. Liu and S. Yang, Journal of Materials Chemistry **22** (15), 7461 (2012).
19. D. Pan, L. Guo, J. Zhang, C. Xi, Q. Xue, H. Huang, J. Li, Z. Zhang, W. Yu, Z. Chen, Z. Li and M. Wu, Journal of Materials Chemistry **22** (8), 3314 (2012).
20. K. Habiba, V. I. Makarov, J. Avalos, M. J. F. Guinel, B. R. Weiner and G. Morell, Carbon **64**, 341-350 (2013).
21. K. A. Ritter and J. W. Lyding, Nat Mater **8** (3), 235-242 (2009).
22. J. Fernández-Rossier and J. Palacios, Physical Review Letters **99** (17) (2007).
23. J. Guttinger, F. Molitor, C. Stampfer, S. Schnez, A. Jacobsen, S. Droscher, T. Ihn and K. Ensslin, Reports on progress in physics. Physical Society **75** (12), 126502 (2012).
24. B. Mandal, S. Sarkar and P. Sarkar, Journal of Nanoparticle Research **14** (12) (2012).
25. K. Nakada, M. Fujita, G. Dresselhaus and M. S. Dresselhaus, Physical Review B **54** (24), 17954-17961 (1996).

26. C. Stampfer, S. Fringes, J. Güttinger, F. Molitor, C. Volk, B. Terrés, J. Dauber, S. Engels, S. Schnez, A. Jacobsen, S. Dröscher, T. Ihn and K. Ensslin, Frontiers of Physics **6** (3), 271-293 (2011).
27. W. L. Wang, S. Meng and E. Kaxiras, Nano Lett **8** (1), 241-245 (2008).
28. Y. Dong, H. Pang, S. Ren, C. Chen, Y. Chi and T. Yu, Carbon **64**, 245-251 (2013).
29. L.-L. Li, J. Ji, R. Fei, C.-Z. Wang, Q. Lu, J.-R. Zhang, L.-P. Jiang and J.-J. Zhu, Advanced Functional Materials **22** (14), 2971-2979 (2012).
30. Y. Li, Y. Hu, Y. Zhao, G. Shi, L. Deng, Y. Hou and L. Qu, Advanced materials **23** (6), 776-780 (2011).
31. D. Pan, J. Zhang, Z. Li and M. Wu, Advanced materials **22** (6), 734-738 (2010).
32. J. Peng, W. Gao, B. K. Gupta, Z. Liu, R. Romero-Aburto, L. Ge, L. Song, L. B. Alemany, X. Zhan, G. Gao, S. A. Vithayathil, B. A. Kaipparettu, A. A. Marti, T. Hayashi, J. J. Zhu and P. M. Ajayan, Nano Lett **12** (2), 844-849 (2012).
33. J. Lee, K. Kim, W. I. Park, B. H. Kim, J. H. Park, T. H. Kim, S. Bong, C. H. Kim, G. Chae, M. Jun, Y. Hwang, Y. S. Jung and S. Jeon, Nano Lett **12** (12), 6078-6083 (2012).
34. S. J. Wang, Z. G. Chen, I. Cole and Q. Li, Carbon **82**, 304-313 (2015).
35. G. Eda, Y. Y. Lin, C. Mattevi, H. Yamaguchi, H. A. Chen, I. S. Chen, C. W. Chen and M. Chhowalla, Advanced materials **22** (4), 505-509 (2010).
36. D. B. Shinde and V. K. Pillai, Chemistry **18** (39), 12522-12528 (2012).
37. S. Zhu, J. Zhang, X. Liu, B. Li, X. Wang, S. Tang, Q. Meng, Y. Li, C. Shi, R. Hu and B. Yang, RSC Advances **2** (7), 2717 (2012).
38. L. B. Tang, R. B. Ji, X. K. Cao, J. Y. Lin, H. X. Jiang, X. M. Li, K. S. Teng, C. M. Luk, S. J. Zeng, J. H. Hao and S. P. Lau, Acs Nano **6** (6), 5102-5110 (2012).
39. J. Biscoe, Journal of Applied Physics **13** (6), 364 (1942).
40. T. Ungar, J. Gubicza, G. Ribarik, C. Pantea and T. W. Zerda, Carbon **40** (6), 929-937 (2002).
41. B. E. Warren, Phys Rev **59** (9), 693-698 (1941).
42. A. Manivannan, M. Chirila, N. C. Giles and M. S. Seehra, Carbon **37** (11), 1741-1747 (1999).
43. F. Tuinstra, The Journal of Chemical Physics **53** (3), 1126 (1970).
44. Z. Y. Li, W. H. Zhang, Y. Luo, J. L. Yang and J. G. Hou, J Am Chem Soc **131** (18), 6320(2009).
45. T. Sun and S. Fabris, Nano Lett **12** (1), 17-21 (2012).
46. E. F. Sheka and L. A. Chernozatonskii, Int J Quantum Chem **110** (10), 1938-1946 (2010).
47. S. Fujii and T. Enoki, Accounts Chem Res **46** (10), 2202-2210 (2013).